ELSEVIER

Nuclear Instruments and Methods in Physics Research A 482 (2002) 79–93

NUCLEAR INSTRUMENTS & METHODS IN PHYSICS RESEARCH Section A

www.elsevier.com/locate/nima

High resolution beam line for the Grand Raiden spectrometer

T. Wakasa[a,*], K. Hatanaka[a], Y. Fujita[b], G.P.A. Berg[a,c], H. Fujimura[a], H. Fujita[b], M. Itoh[d], J. Kamiya[a], T. Kawabata[d,1], K. Nagayama[a], T. Noro[a,2], H. Sakaguchi[d], Y. Shimbara[b], H. Takeda[d], K. Tamura[e], H. Ueno[b,3], M. Uchida[d], M. Uraki[a], M. Yosoi[a]

[a] *Research Center for Nuclear Physics, Osaka University, Mihogaoka 10-1, Ibaraki, Osaka 567-0047, Japan*
[b] *Department of Physics, Osaka University, Machikaneyama 1-1, Toyonaka, Osaka 560-0043, Japan*
[c] *Indiana University Cyclotron Facility, Bloomington, IN 47405, USA*
[d] *Department of Physics, Kyoto University, Kitashirakawa, Sakyo, Kyoto 606-8502, Japan*
[e] *Department of Physics, Fukui Medical University, Himoaitsuki 23-3, Matsuoka, Fukui 910-1193, Japan*

Received 20 March 2001; received in revised form 20 July 2001; accepted 21 July 2001

Abstract

We have designed and constructed a new beam line which can accomplish both lateral and angular dispersion matching with the Grand Raiden spectrometer. In dispersive mode, lateral and angular dispersions of the beam line are $b_{16} = 37.1$ m and $b_{26} = -20.0$ rad, respectively, to satisfy matching conditions for Grand Raiden. In achromatic mode, the beam line satisfies the double achromatic condition of $b_{16} = b_{26} = 0$. The magnifications of the beam line are $(M_x, M_y) = (-0.98, 0.89)$ and $(-1.00, -0.99)$ for dispersive and achromatic modes, respectively. In the commissioning experiments, we have succeeded to separate the first excited 2^+ state of ^{168}Er with $E_x = 79.8$ keV clearly from the ground state in the (p, p') reaction. We achieved energy resolutions of $\Delta E = 13.0 \pm 0.3$ and 16.7 ± 0.3 keV in full width at half-maximum for 295 and 392 MeV protons, respectively. These energy resolutions agree with the resolving power of Grand Raiden for an object size of about 1 mm.

PACS: 29.27.Eg; 29.30.Aj; 20.30.Ep

Keywords: Dispersion matching; Beam transport; Magnetic spectrometer; (p, p') Reaction

1. Introduction

The spectroscopy of charged particles provides a potentially rich source of nuclear structure information, and extensive studies have been performed with (p, p') and $(^3He, t)$ reactions. The RCNP AVF [1] and Ring [2] Cyclotrons can deliver polarized proton beams up to $T_p = 400$ MeV as well as ^{3}He beams up to $T_{^3He} = 540$ MeV (180 MeV/A). The RCNP facility has the magnetic spectrometer

*Corresponding author. Tel.: +81-6-6879-8935; fax: +81-6-6879-8899 *URL*: http://www.rcnp.osaka-u.ac.jp/~wakasa (T. Wakasa).

E-mail address: wakasa@rcnp.osaka-u.ac.jp (T. Wakasa).

[1] Present address: Research Center for Nuclear Physics, Osaka University, Mihogaoka 10-1, Ibaraki, Osaka 567-0047, Japan.

[2] Present address: Department of Physics, Kyushu University, Hakozaki 6-10-1, Higashi, Fukuoka 812-8581, Japan.

[3] Present address: The Institute of Physical and Chemical Research, Hirosawa 2-1, Wako, Saitama 351-0198, Japan.

0168-9002/02/$ - see front matter
PII: S0168-9002(01)01686-2

Grand Raiden [3]. It is characterized by its high resolving power R of about 37,000 for a monochromatic beam spot size of 1 mm. The Grand Raiden spectrometer can analyze particles with a maximum rigidity of $B\rho = 5.4$ Tm which corresponds to $T_t = 450$ MeV (150 MeV/A) for tritons.

Recently, a focal plane polarimeter system [4] has been constructed for Grand Raiden to measure a complete set of polarization transfer observables (D_{ij}) for the $(\vec{p},\vec{p}')$ reaction in the energy range of $T_p = 200$–400 MeV. In this intermediate energy region, the D_{ij} observables for proton inelastic scattering provide a sensitive filter for studies of nuclear spin responses [5]. Furthermore at projectile energies above 100 MeV/A, due to the energy dependence of the isovector part of the t-matrices [6], the (^{3}He, t) charge exchange reaction excites predominantly the spin–isospin excitations in nuclei [7]. Thus, the RCNP Ring Cyclotron Facility is a unique facility for nuclear spectroscopic studies emphasizing spin degrees of freedom.

The intrinsic momentum resolution of Grand Raiden is given by $\Delta p/p = 1/R = |M_x/D|\Delta x_0$ with Δx_0 being the monochromatic beam size on target, and M_x and D the magnification and dispersion of the spectrometer. Thus, for $\Delta x_0 = 1$ mm, the expected momentum resolution should be $\Delta p/p = 2.7 \times 10^{-5}$ corresponding to an energy resolution of about 18 keV for 400 MeV protons. However, the typical energy resolution achieved with Grand Raiden and the previous WN beam line was about 120 keV [8]. This was mainly governed by the energy spread of the incident beam.

The demand for higher resolution necessary for nuclear spectroscopy led to the design and construction of the new beam line (WS beam line) [9] connecting the Ring Cyclotron and the Grand Raiden spectrometer. The beam line should be designed so that the momentum spread of the beam does not limit the final resolution. This can be achieved by lateral dispersion [10] and focus [9,11] matching between the beam line and spectrometer in addition to kinematic displacement of the spectrometer. Furthermore, the WS beam line is designed to realize angular dispersion matching [9] which is important to determine the reaction angle with high accuracy.

In Section 2, we present a brief description for the Grand Raiden spectrometer and detector system. In Section 3, we will describe the lateral and angular dispersion matching method. In Section 4, the design concept of the WS beam line will be presented.

In Sections 5 and 6, we will describe the specifications of the WS beam line and its ion-optical properties in dispersive and achromatic modes. Sections 7 and 8 are devoted to recent experimental results with the new beam line. A summary is given in Section 9.

2. The Grand Raiden spectrometer and detector system

The magnetic spectrometer Grand Raiden [3] was designed and constructed for high resolution spectroscopy at the RCNP Ring Cyclotron Facility. The spectrometer consists of two dipole (D1 and D2) magnets, two quadrupoles (Q1 and Q2), a sextupole (SX), and a multipole (MP) as shown in Fig. 1. The function of the sextupole is to satisfy second-order ion-optical requirements, namely, to

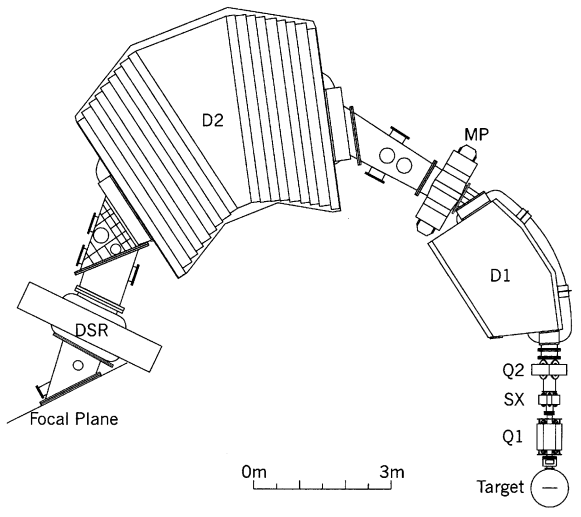

Fig. 1. A schematic layout of the Grand Raiden spectrometer at RCNP.

provide a focal plane tilting angle of $\Phi_x = 45^\circ$ and $(x|\theta^2) = (x|\phi^2) = 0$. The multipole at the exit of D1 can generate magnetic fields with quadrupole, sextupole, octupole, and decapole components. These fields are used to compensate ion-optical aberrations of the system. It should be noted that Berz et al. [12] have proposed another method to eliminate these higher-order and aberration effects on the final position and angle resolutions. This method uses a high order transfer map of a spectrometer, and has been applied at the S800 spectrometer at the National Superconducting Cyclotron Facility [12] as well as at the Hall A high resolution spectrometer at the Thomas Jefferson National Accelerator Facility [13,14].

An additional dipole (DSR) magnet is installed at the end of the spectrometer for rotating in-plane components of the polarization vector for protons. This rotation enables us to measure these components with the focal plane polarimeter [4] downstream of the focal plane detector system.

Table 1 summarizes the ion-optical properties of the Grand Raiden spectrometer. The spectrometer is characterized by a high resolving power of $R = 37{,}000$. A detailed description of the spectrometer can be found in Ref. [3].

The positions and angles of particles analyzed by the spectrometer are measured by a detector system in the focal plane. This system consists of two sets of vertical drift chambers (VDC's) [15] with two anode-wire planes (x and u planes) followed by a pair of plastic scintillators. Wires of the x-plane are stretched vertically, while those of the u-plane are tilted by an angle of $+48.2^\circ$ relative to the vertical direction. Horizontal and vertical positions as well as the angles are determined using the measured drift times of the ionization charges collected on the anode wires of the x and u planes. Thus, by combining the information from the x and u planes, each VDC can separately reconstruct particle rays. This redundant information was used to measure the position resolution of the detector system. The position resolution is better than 0.35 mm in full-width at half-maximum (FWHM) [16].

Table 1
Ion-optical properties of the Grand Raiden spectrometer[a]

Matrix elements	Design values
$M_x = (x\|x)$	-0.417
$M_y = (y\|y)$	5.98
$D = (x\|\delta)$	15.451 m
$\Phi_x = \tan^{-1}[-(x\|\theta\delta)M_x/D]$	45°

[a] The matrix elements $(x|\theta) = (y|\phi) = (x|\theta^2) = (y|\phi^2) = 0$.

The smallest beam size at the object point after the Ring Cyclotron is about 1 mm. The magnification of the new WS beam line in dispersive mode is $M_x = -0.98$, and the monochromatic beam spot size at the target position is, therefore, expected to be about 1 mm, too. With the spectrometer magnification of $M_x = -0.417$, this results in a smallest focal plane image of about 0.4 mm. The detector resolution is therefore sufficient to resolve spectra up to the resolving power limit of $\Delta p/p = 2.7 \times 10^{-5}$ corresponding to 18 keV at 400 MeV protons as mentioned above.

3. Matching between a beam line and a spectrometer

Cohen [10] proposed for the first time the concept of "dispersion matching". He showed that, if the beam line and a spectrometer are properly "matched", the spectral resolution can be better than the momentum spread of the beam up to limit of the resolving power of the analyzing spectrometer. This concept was demonstrated by Blosser et al. [17]. Subsequently, many facilities with magnetic spectrometers have adopted and realized this technique [11,12,18,19]. At these facilities, the resolving power of the spectrometer was significantly better than the momentum spread of the incident beam. The dispersion matching conditions were achieved with a suitable beam transport system, and the momentum spread of the beam was compensated. Detailed descriptions concerning the dispersion matching method can be found in Refs. [11,18,19]. In the following, therefore, we summarize a description of this method.

Following the notation of the computer code TRANSPORT [20], the position x and angle θ in the focal plane position can be described in first

order with the matrix elements of b_{ij} and s_{ij} of the beam line and the spectrometer, respectively, as

$$\begin{aligned} x = &(s_{11}b_{11}T + s_{12}b_{21})x_0 \\ &+ (s_{11}b_{12}T + s_{12}b_{22})\theta_0 \\ &+ (s_{11}b_{16}T + s_{12}b_{26} + s_{16}C)\delta_0 \\ &+ (s_{12} + s_{16}K)\Theta \end{aligned} \quad (1)$$

$$\begin{aligned} \theta = &(s_{21}b_{11}T + s_{22}b_{21})x_0 \\ &+ (s_{21}b_{12}T + s_{22}b_{22})\theta_0 \\ &+ (s_{21}b_{16}T + s_{22}b_{26} + s_{26}C)\delta_0 \\ &+ (s_{22} + s_{26}K)\Theta. \end{aligned} \quad (2)$$

where x_0, θ_0, and δ_0 are the position, angle, and fractional momentum deviations from the central trajectory at the exit of the Ring Cyclotron, respectively. The suffixes 1, 2, and 6 of b_{ij} and s_{kl} represent the coordinates of position, angle, and fractional momentum, respectively. The angle Θ is the relative scattering angle, T the target function, K and C describe the kinematic factors. Details for these factors can be found in Ref. [11].

The aim of beam line matching is to give the best resolving power in the system including the beam line. This is achieved by minimizing the image size of x by eliminating the coefficients of θ_0, δ_0, and Θ in Eq. (1). If the angle information is important, "angular" dispersion matching has to be achieved by minimizing the coefficient of δ_0 in Eq. (2). Since a large dispersion b_{16} of the beam line is required for the lateral dispersion matching as described below, the δ_0 dependence of θ becomes large. Therefore, the angular dispersion matching is very important in order to eliminate the ambiguity coming from δ_0 when the scattering angle Θ is to be determined from the measured θ in the focal plane.

The conditions for lateral and angular dispersion matching can be satisfied simultaneously [9] by setting the matrix elements of the beam line to be

$$b_{12} = -\frac{s_{12}}{s_{11}}b_{22}T \quad (3)$$

$$b_{16} = -\frac{s_{16}}{s_{11}}(1 + s_{11}s_{26}K - s_{21}s_{16}K)\frac{C}{T} \quad (4)$$

$$b_{26} = (s_{21}s_{16} - s_{11}s_{26})C \quad (5)$$

and by setting those of the spectrometer to be

$$s_{12} = -s_{16}K. \quad (6)$$

4. Requirements and design concept

We consider the beam line requirements for lateral and angular dispersion matching with the Grand Raiden spectrometer. We assume $K = 0$ and $C = T = 1$ for simplicity.

4.1. Ion-optical requirement

Table 1 summarizes the ion-optical properties of Grand Raiden. By using these values, the lateral and angular dispersion matching conditions in Eqs. (3)–(5) can be evaluated to be

$$b_{12} = 0 \quad (7)$$

$$b_{16} = -\frac{s_{16}}{s_{11}} = 37.1 \text{ m} \quad (8)$$

$$b_{26} = s_{21}s_{16} - s_{11}s_{26} = -20.0 \text{ rad} \quad (9)$$

where we have used $s_{12} = -s_{16}K = 0$ in Eq. (6).

With the previous WN beam line [21], it was hard to satisfy the lateral dispersion matching condition, and there was no capability of the angular dispersion matching. Thus we have decided to design a new beam line and replace this beam line with the new WS beam line which can fulfill the lateral and angular dispersion matching conditions in particular to reach the resolving power limit of the Grand Raiden spectrometer.

4.2. Requirement for beam line polarimeters

The WS beam line transports the beam from the object point at the exit of the Ring Cyclotron (BV-EXT) to the target position. In this line, there are at least two double-focusing locations for both required beam line polarimeters. The polarimeters for polarized proton and deuteron beams make use of the analyzing powers of the elastic scatterings on hydrogen. The elastically scattered particles and recoil protons are detected in a kinematical coincidence with a conjugate-angle

pair of plastic scintillators. A self-supporting CH_2 target is used as a hydrogen target.

Each individual polarimeter can only measure the normal and sideways components of a polarization vector. In order to determine the longitudinal polarization component, two sets of polarimeters separated with an appropriate bending angle are needed. For the optimal spin precession angle of 270°, the corresponding bending angles are 106° and 124° for 400 and 200 MeV protons, respectively. Most experiments at RCNP have been performed in this energy range, and the present bending angle of 115° between polarimeters is a compromise which covers this region.

4.3. Ion-optical design concept

The beam is transported through several dipole and quadrupole magnets. The dipole magnets are tuned to pass the beam through the central orbit, while the quadrupole magnets are tuned to focus the diverging beam. Two quadrupole magnets are enough to focus the beam in both the horizontal and vertical planes. Thus we designed the WS beam line to have only two parameters between the focusing points where the beam viewers are positioned. If there are more than two quadrupole magnets between the points, we have grouped them in pairs, and the current setting for the magnets in a group is the same.

5. Description of WS beam line

The layout of the WS beam line is shown in Fig. 2. It consists of five sections with dipole and/or quadrupole magnets as well as one special quadrupole magnet QM9S. A section extends from one double-focus to the next. In section I, the beam is bent 40° from the object point at the exit of the Ring Cyclotron (BV-EXT) and is transported to the first double-focusing point Beam Line Polarimeter I (BLP1). The beam is bent clockwise through 115° in section II and is

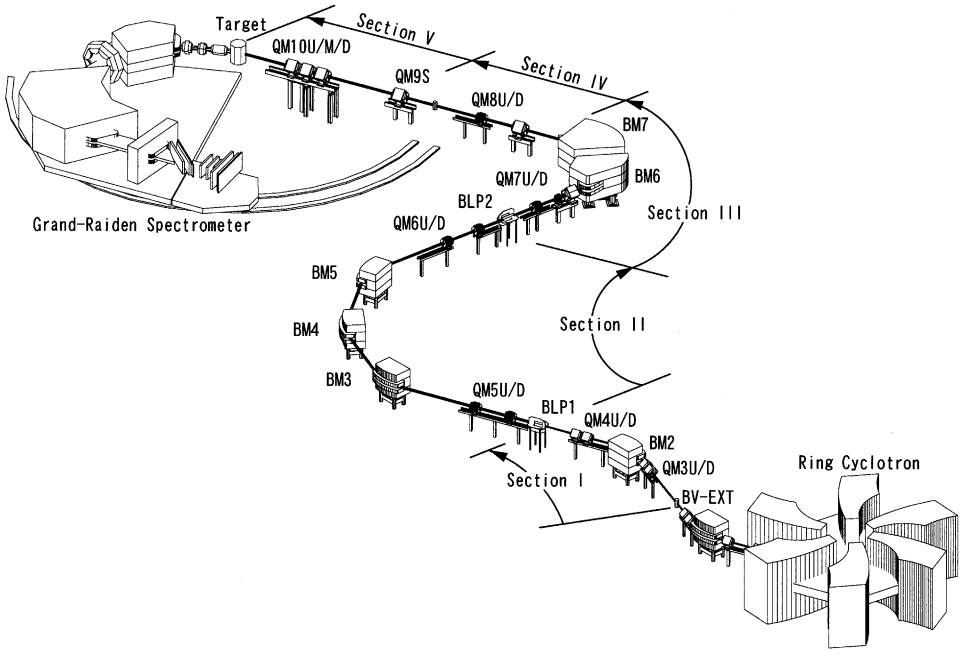

Fig. 2. A schematic view of the WS beam line at RCNP from the object point at the Ring Cyclotron exit (BV-EXT) to the target position of the Grand Raiden spectrometer. There are five dipole and 16 quadrupole magnets labeled BM*n* and QM*n*U/M/D/S, respectively. The beam line polarimeters BLP1 and BLP2 are positioned at double-focus locations of the beam line.

focused on the second double-focusing point Beam Line Polarimeter II (BLP2). Subsequently, the beam is bent counterclockwise through 115° in section III. Sections IV and V are the straight sections to the target point, and the QM9S magnet is between them at an intermediate focus. In the following, we describe the properties and specifications of each section as well as of the complete system after summarizing the specifications of dipole and quadrupole magnets used in the beam line.

5.1. Dipole and quadrupole magnets

The specifications of dipole magnets are listed in Table 2 [22]. Three B40C dipole magnets with a bending angle of 40° and a B30C dipole magnet with a bending angle of 30° are installed in sections I and II of the beam line. All magnets were existing and recovered from the previous beam line and originally had a magnet gap of 70 mm. Two of the B40C magnets and the B30C magnet were modified to have a magnet gap of 60 mm in order to extend the good-field region with constant dipole field.

The other two dipole magnets, D1 and D2, have been transferred from IUCF to RCNP for the construction of the WS beam line. These magnets were formerly used as a part of the K600 spectrometer at IUCF [19]. The specifications of these magnets are also summarized in Table 2. The H and K coils used for the kinematical and sextupole corrections were removed since they are not needed in the WS beam line.

The specifications of the quadrupole magnets are listed in Table 3 [22]. Three types of magnets are used depending on the requirements for aperture (small, middle, and large) and field strengths.

5.2. Description of beam line sections

Section I includes the beam line from the object point after the Ring Cyclotron (BV-EXT) to the first double-focusing point where the first beam line polarimeter BLP1 is installed. This section consists of one B40C magnet (BM2) with a gap of 70 mm and four small aperture quadrupole magnets (QM3U/D and QM4U/D). We have grouped these quadrupole magnets in pairs. One group of QM3U and QM4D acts as the vertically focusing element, while the other of QM3D and QM4U functions as horizontal focusing. The magnifications and dispersion of this section are $(M_x, M_y) = (-0.75, -1.33)$ and $D = 2.94$ m. Thus $|D/M_x|$ is 3.94 m.

Section II extends from BLP1 to the next double-focusing point where the second beam line polarimeter BLP2 is positioned. This section consists of two B40C magnets (BM3 and BM5) and one B30C magnet (BM4) with a gap of

Table 3
Specifications of the quadrupole magnets in the WS beam line

	Aperture		
	Small	Middle	Large
Aperture	70 mm	106 mm	114 mm
Pole length	400 mm	250 mm	400 mm
Maximum field gradient	20 T/m	9 T/m	14 T/m

Table 2
Specifications of the dipole magnets in the WS beam line before modification

	B40C	B30C	D1	D2
Magnet gap	70 mm	70 mm	100 mm	80 mm
Radius	2185.5 mm	2185.5 mm	2100 mm	2100 mm
Bending angle	40°	30°	55°	60°
Edge angle at entrance	20°	15°	−10°	0°
Edge angle at exit	20°	15°	0°	10°
Maximum field strength	1.46 T	1.46 T	1.74 T	1.74 T

60 mm, and four middle aperture quadrupole magnets (QM5U/D and QM6U/D). The total bending angle of this section should be 115° in order to match the bending angle of the following section with the D1 and D2 magnets. Thus the bending angles of B40C and B30C were changed to 41.5° and 32.0° from the original values of 40.0° and 30.0°, respectively. As a result, bending radii of B40C and B30C were modified to 2109.8 and 2065.8 mm, respectively, from the original value of 2185.5 mm. The four quadrupole magnets are grouped in pairs. One group of QM5U and QM6D acts as the vertically focusing element, while the other consisting of QM5D and QM6U is horizontally focusing. The magnifications and dispersion of this section are $(M_x, M_y) = (-1.00, 1.00)$ and $D = 12.5$ m. Thus $|D/M_x|$ becomes 12.5 m.

Section III starts at BLP2 and continues to the third double-focusing point at the exit of BM7. This section consists of the two dipole magnets D1 and D2 (BM6 and BM7), one middle aperture quadrupole magnet (QM7U), and one large aperture quadrupole magnet (QM7D). The QM7U quadrupole is used only in achromatic mode. The QM7D acts as the vertically focusing element, while the rotation of the entrance pole-face of BM6 provides the needed horizontal focusing. The magnifications and dispersion of this section are $(M_x, M_y) = (-0.30, -1.58)$ and $D = 3.85$ m. Thus $|D/M_x|$ becomes 12.9 m.

Section IV transports the beam from the end of section III to the fourth double-focusing location. This section consists of one large aperture quadrupole magnet (QM8U) and one middle aperture quadrupole magnet (QM8D). The QM8U and QM8D magnets provide horizontal and vertical focusing, respectively. The main function of this section is to increase the dispersion produced by sections I, II, and III for the matching required for Grand Raiden. The magnifications of this section are $(M_x, M_y) = (-5.60, -0.55)$.

The quadrupole QM9S is positioned at the fourth double-focusing point. At this point the beam is focused both horizontally and vertically. The horizontal beam size is dominated by the large dispersion of 47.3 m and the momentum spread of the beam. Thus this quadrupole can change the correlation between the momentum and the horizontal angle of the beam while the other ion-optical properties such as the dispersion are nearly unchanged. These functions are necessary for the angular dispersion matching for which the angular dispersion b_{26} should be controlled independently of other beam properties.

Section V transports the beam from QM9S to the fifth and last double-focusing point where the target is positioned. This section consists of a set of symmetric triplet quadrupole magnets with large aperture. The QM10U and QM10D magnets act as horizontally focusing elements, while QM10M provides vertical focusing. The main function of this section is to focus the beam downstream of the target as required by the focusing condition.

5.3. Overall dispersive beam line performance

The ion-optical properties and specifications of the WS beam line are summarized in Table 4. It should be noted that the beam line has nominal lateral and angular dispersions of $b_{16} = 37.1$ m and $b_{26} = -20.0$ rad necessary to satisfy dispersion matching conditions for Grand Raiden. These dispersions can be varied as required by matching conditions for different kinematical conditions. The nominal magnifications are $(M_x, M_y) = (-0.98, 0.89)$.

Fig. 3 shows several horizontal and vertical first order beam rays for the WS beam line and the Grand Raiden spectrometer. The beam is focused in both the horizontal and vertical planes at the

Table 4
Ion-optical properties of the WS beam line

Matrix elements	Design values	
	Dispersive mode	Achromatic mode
$b_{11} = (x\|x)$	−0.98	−1.00
$b_{33} = (y\|y)$	0.89	−0.99
$b_{16} = (x\|\delta)$	37.1 m	0
$b_{26} = (\theta\|\delta)$	−20.0 rad	0
$b_{12} = (x\|\theta)$	0	0
$b_{34} = (y\|\phi)$	0	0
Total bending angle	270°	
Total length	65.46 m	

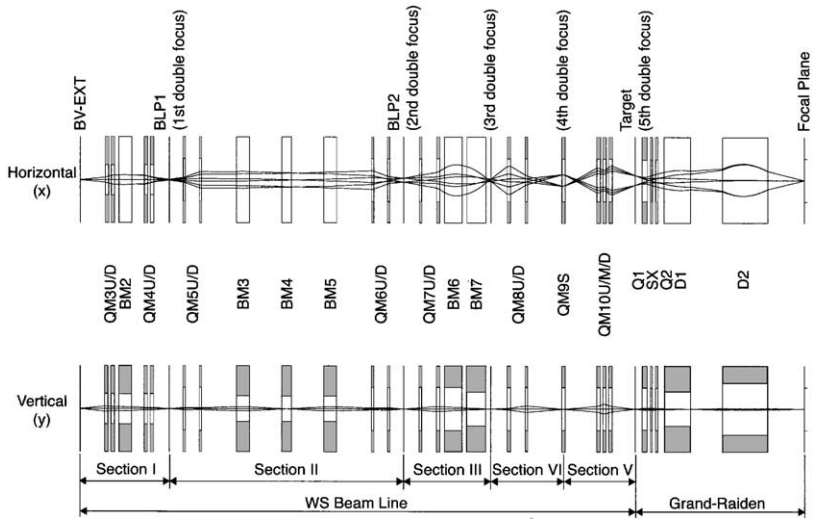

Fig. 3. Envelopes of dispersive beam in the horizontal and vertical planes from the object point at the exit of the Ring Cyclotron (BV-EXT) via the target location to the focal plane of the Grand Raiden spectrometer. Trajectories are shown for particles with $\Delta p/p = \pm 0.03\%$, $\Delta\theta = \pm 2$ mrad, and $\Delta\phi = \pm 2$ mrad. The transverse scale is increased for illustration purposes.

end of each section as described above. Because we modified the dipole magnets in section II to a small gap of 60 mm to increase the magnetic good-field region, a small vertical beam envelope is required here. This requirement was fulfilled by focusing the beam vertically at the center of BM4 in section II as shown in Fig. 3.

6. Achromatic beam line mode

In addition to dispersive mode, the WS beam line is designed to be able to deliver also a double-achromatic beam with zero lateral and angular dispersions. In the following we summarize how to realize the double-achromatic beam transport by appropriate settings of the quadrupole magnets.

6.1. Achromatic tune of beam line sections

Section I in achromatic mode has a different setting as in dispersive mode. There is a vertically focusing location at the exit of BM2. This vertical focus is realized by the doublet consisting of the QM3U and QM3D quadrupole magnets. The following QM4U and QM4D magnets act as the vertically and horizontally focusing elements, respectively, and the beam is doubly focused at BLP1. The magnifications and dispersion of this section are $(M_x, M_y) = (-1.47, 1.36)$ and $D = 1.48$. Thus $|D/M_x|$ becomes 1.01.

Section II has a double-focusing point inside the BM4 bending magnet. The four quadrupole magnets are grouped in pairs. One group of QM5U and QM6D acts as vertical focusing, while the other consisting of QM5D and QM6U functions as horizontal focusing. The magnifications and dispersion of this section are $(M_x, M_y) = (1.00, 1.00)$ and $D = 0$. Thus $|D/M_x|$ is 0.

Sections III and IV act as one ion-optical unit. The beam is transported from BLP2 to a location slightly upstream of QM9S where the beam is doubly focused. The four quadrupole magnets are grouped in pairs. One group of QM7U and QM8D acts as horizontal focusing, while the other QM7D and QM8U functions as vertical focusing. The magnifications and dispersion of this section are $(M_x, M_y) = (0.47, 1.90)$ and $D = 0.70$. The lateral dispersion produced by section I is compensated in this section. It should be noted that the angular dispersion produced by sections I and II is also cancelled.

The last section consists of QM9S and the section V in dispersive mode (see Fig. 2). In

achromatic mode, the QM10U quadrupole is not excited. The remaining three quadrupole magnets are grouped in pairs. One group consisting of QM9S and QM10D acts as horizontal focusing, while the QM10M magnet focuses vertically. These quadrupoles are used to focus the beam both horizontally and vertically at the target location.

6.2. Overall achromatic beam line performance

In Fig. 4, the horizontal and vertical first-order beam envelopes are shown for the WS beam line and the Grand Raiden spectrometer. The double-achromatic transport is realized at the target location, i.e. $b_{16} = b_{26} = 0$ with the double focusing conditions of $b_{12} = b_{34} = 0$. Special care has been taken to make the magnification close to unity. The magnifications of the beam line are $(M_x, M_y) = (-1.00, -0.99)$.

7. Beam line setting and dispersion matching

In the following, we briefly describe how the WS beam line is set and optimized for dispersion matching by using the Grand Raiden spectrometer as diagnostic system.

Firstly, dipole fields of all magnets in the WS beam line are set by the currents according to the rigidity ($B\rho$ value) of the beam to be transported. For reproducibility, the magnets are always driven to the desired field levels through saturation. Then the current settings are fine-tuned in order to pass the beam through the center of the following quadrupole magnets. The ion-optical calculations give field strengths of quadrupole magnets. Then currents of these magnets are set as calculated from measured calibrations.

After these coarse settings of the currents, fine tuning of the currents for quadrupole magnets described below is necessary in order to realize the lateral and angular dispersion matching.

At first, quadrupole magnets in beam line sections I, II, and III are roughly adjusted with the help of beam viewers in order to provide a double-focus of the beam at the end of each section. Then the fine tuning of sections IV and V as well as of QM9S is performed by using the faint-beam method to satisfy the double-achromatic condition in the focal plane of Grand Raiden. A detailed description of this method can be found in Refs. [23,24].

In the faint-beam method, the attenuated faint-beam is transmitted through the Grand Raiden

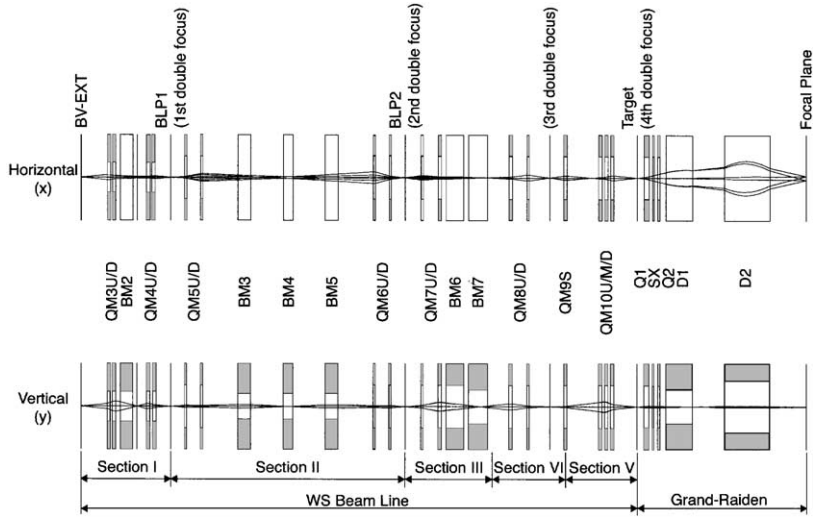

Fig. 4. WS beam line in achromatic mode. For details, see legend of Fig. 3.

spectrometer and measured by the focal plane detectors. The lateral and angular dispersion matching conditions for $K = 0$ and $C = 1$ mean that the transmitted beam should satisfy the double-achromatic conditions after being analyzed by the spectrometer. These conditions can be verified by using the position and angle information of the focal plane detectors. The lateral and angular dispersions of the WS beam line and Grand Raiden are matched by minimizing the width of position and angle of the beam distribution in the focal plane.

In this method, the quadrupole magnets of QM10U/M/D are at first tuned to minimize the width of the position in the focal plane. This means that the beam is focused at the target position. Then the lateral and angular dispersions of the beam line are changed by using QM8U in section IV and QM9S until their optimum settings are reached as explained above. Fig. 5 shows the

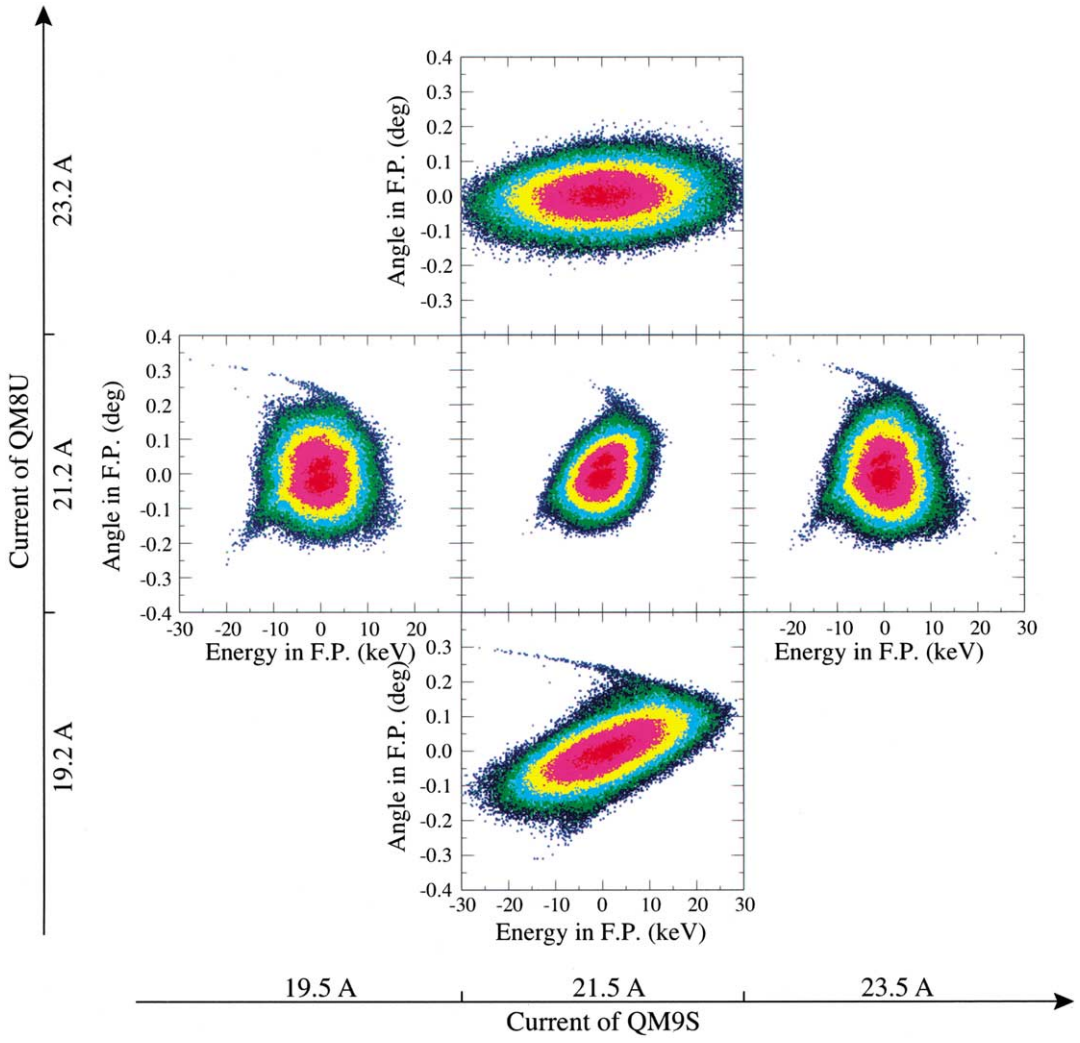

Fig. 5. Horizontal beam profiles in the focal plane of the Grand Raiden spectrometer. The horizontal axis shows the energy of the particle analyzed by the spectrometer relative to the mean energy of the beam. The vertical axis shows the angle of the particle in the focal plane (FP). From left to right, results with three different currents of QM9S are shown. From top to bottom, results with three different currents of QM8U are shown.

energy and angle spectra of the transmitted beam in the focal plane. The results for five different settings of QM8U and QM9S are shown. In this case, the lateral and angular dispersion matching conditions were satisfied simultaneously with the current settings of QM8U = 21.2 A and QM9S = 21.5 A for 295 MeV protons.

The WS beam line is designed so that the beam is focused in the center of QM9S. Since the beam is focused, we can change the angular dispersion with QM9S without noticeably changing the lateral dispersion of the beam line. Figs. 6 and 7 show the energy and angle widths of the transmitted beam in the focal plane, respectively, as a function of the current setting of QM9S. In this case, the lateral and angular dispersion matching conditions were satisfied simultaneously with the current setting of QM9S = 21.5 A. The minimum of the angle width is about $\Delta\theta = 0.16^\circ$ (2.8 mrad) which corresponds to the beam emittance $\Delta\theta_0 = s_{11}b_{11}\Delta\theta$ of 1.1 mrad. The angle width is changed as a function of the current setting (Fig. 7), while the position width is almost constant in this region (Fig. 6). In Fig. 6, the energy width as a function of the current setting of QM8U is also shown by the filled circles. The QM8U magnet changes the dispersion of the beam line. Therefore, the energy width is sensitive to the current setting of QM8U, which is in contrast to the insensitivity to the current setting of QM9S. This demonstrates clearly that lateral and angular dispersions in this beam line can be controlled almost independently with QM8U and QM9S magnets, respectively. Finally, sections I, II, and III are fine-tuned to give a minimum width of the transmitted beam in the focal plane. This fine-tuning ensures the focus of the beam at the end of each section is as designed.

8. Measurements

Since April 2000, when the WS beam line was commissioned, the system was used for a variety of nuclear physics experiments. Measurements have been performed with various particle beams of $\vec{p}$, $\vec{d}$, ^{3}He, ^{4}He, etc., in a wide energy range. Energy resolutions of $\Delta E/E = 5 \times 10^{-5}$ and better are possible in dispersive mode. On the other hand, some experiments required only moderate

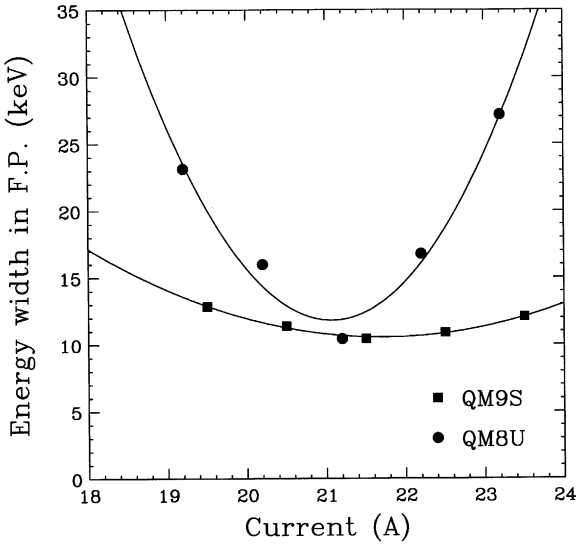

Fig. 6. Energy widths of the beam in dispersive mode in the focal plane (FP) of the Grand Raiden spectrometer as a function of the current of QM9S (filled squares) and QM8U (filled circles). The solid curves are the results of a parabolic fit.

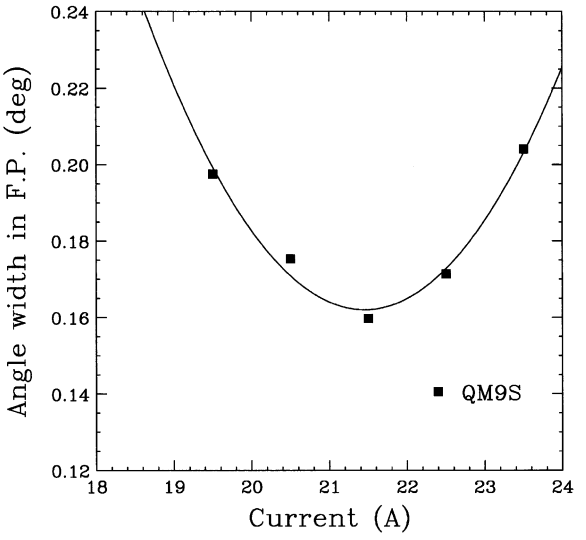

Fig. 7. Angle widths of the beam in dispersive mode in the focal plane (FP) of the Grand Raiden spectrometer as a function of the current of QM9S. The solid curve is the result of a parabolic fit.

resolution and were carried out with $\Delta E/E = 4-8 \times 10^{-4}$ with typical beam currents of several hundreds nA in achromatic mode.

The dispersive mode requires good energy resolution of the beam from the Ring Cyclotron to realize the reasonably small beam spot size at the target. It was demonstrated that the beam spot size has no significant effect on the spectral resolution, but too large a beam spot will create other problem, like the reduction of transmission, target availability and homogeneity. For example, the 150 keV FWHM energy spread of the 400 MeV dispersion-matched proton beam contributes to the spot size at the target position with 10 mm. A relatively good energy resolution of the beam from the Ring Cyclotron can be achieved by tuning the injection line from AVF to Ring Cyclotrons. However, this tuning reduces typical beam currents on target from several hundreds nA to about 10 nA. At present these are the limiting factors for the dispersive beam in high resolution experiments.

The main research activities with the WS beam line in dispersive mode are inelastic scattering [25,26], fine structure of giant resonances [27,28], and transfer reactions for nuclear spectroscopy [29].

In the following, a few examples with the dispersive beam of protons will be presented in order to show the high performance of the WS beam line.

8.1. ^{168}Er(p, p′) *scattering*

Fig. 8 shows the excitation energy spectrum for the ^{168}Er(p, p′) scattering at $T_p = 295$ MeV and $\theta_{lab} = 9^\circ$ [30]. An enriched ^{168}Er target with a thickness of 2 mg/cm^2 was used. The first excited 2^+ state of $E_x = 79.8$ keV is clearly separated from the ground state with an energy resolution of $\Delta E = 13.0 \pm 0.3$ keV in FWHM. The ideal value of the energy resolution can be evaluated from the intrinsic momentum resolution given by $|M_x/D|b_{11}\Delta x_0$. Thus, for the typical Δx_0 value of 1 mm, this value becomes 14 keV for 295 MeV protons which is consistent with the observed value.

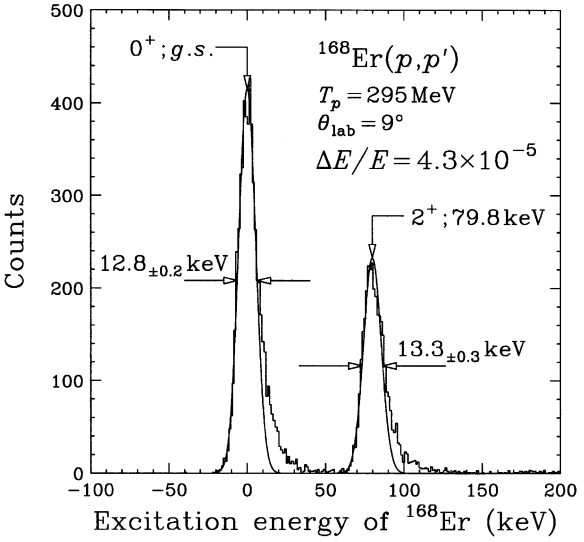

Fig. 8. A typical excitation energy spectrum of the ^{168}Er(p, p′) scattering at $T_p = 295$ MeV and $\theta_{lab} = 9^\circ$ measured with the Grand Raiden spectrometer after employing the dispersion matching method.

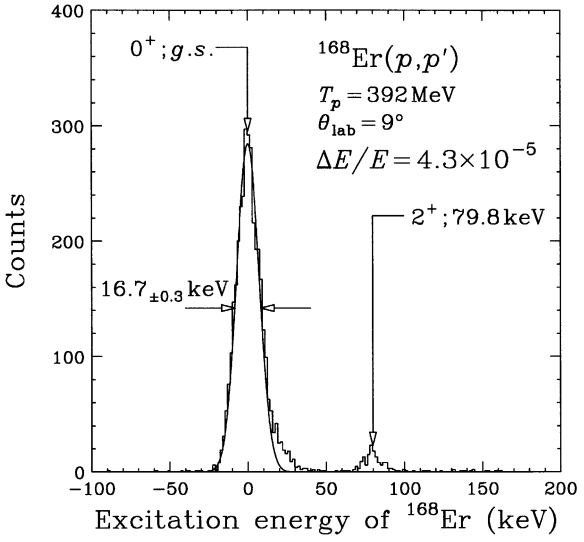

Fig. 9. Same as Fig. 8 but at $T_p = 392$ MeV.

We have also measured a spectrum at $T_p = 392$ MeV and $\theta_{lab} = 9^\circ$, and the result is shown in Fig. 9. In this case the final energy resolution was 16.7 ± 0.3 keV in FWHM which is also consistent with the ideal value of 18 keV for 392 MeV

protons given by the resolving power limit of the spectrometer.

8.2. ^{nat}Si(p, p′) *scattering*

Fig. 10 shows the excitation energy spectrum of the ^{nat}Si(p, p′) reaction at $T_p = 295$ MeV and $\theta_{lab} = 14^\circ$ in the excitation energy range from 5 to 20 MeV. A natural silicon target with a thickness of 1.77 mg/cm^2 was used. This spectrum shows clean separation of individual nuclear level up to about $E_x = 15$ MeV. The observed energy resolution is about 19.1 keV as shown in Fig. 11, an enlargement of levels around $E_x = 10$ MeV. This is significantly worse compared with the ^{168}Er spectrum. This is mainly due to the mismatch in the focus in the focal plane and the increase of the effective magnification coming from the kinematical correction factor $K \neq 0$. The K value is -0.002 for ^{168}Er, while that for silicon is about -0.012. After the kinematical correction of $s_{12} = -s_{16}K$ realized by shifting the focal plane, x in Eq. (1) depends on θ_0 as $x = 0.19\theta_0$. Thus the beam emittance of $\Delta\theta_0 = 1.1$ mrad contributes to Δx with 0.22 mm for ^{nat}Si. Furthermore, the effective magnification of $s_{11}b_{11}T + s_{12}b_{21}$ becomes larger by a factor of 1.2. The contributions from these two effects to the energy resolution are estimated to be about 17 keV which reasonably agrees with the experimental result of 19.1 keV. It should be noted that the dispersion matching is still possible for $K \neq 0$ by using the single-slit method [23,24] instead of the faint-beam method employed here which works only for $K = 0$.

8.3. ^{16}O(p, p′) *scattering*

Fig. 12 shows the excitation energy spectrum of the ^{16}O(p, p′) scattering at $T_p = 295$ MeV and $\theta_{lab} = 14^\circ$ [30]. The spectrum for the ^{16}O(p, p′) scattering was extracted by means of a subtraction of the ^{nat}Si(p, p′) spectrum from the ^{nat}SiO$_2$(p, p′) one. A natural SiO$_2$ target with a thickness of 1.77 mg/cm^2 was used.

Since the mass number of ^{16}O is only about one-half of ^{nat}Si, the energy resolution for ^{16}O is expected to be worse compared with that for ^{nat}Si because of the K-dependence of dispersion matching which was not corrected as in the ^{nat}Si case. The observed energy resolution is about 22.0 keV

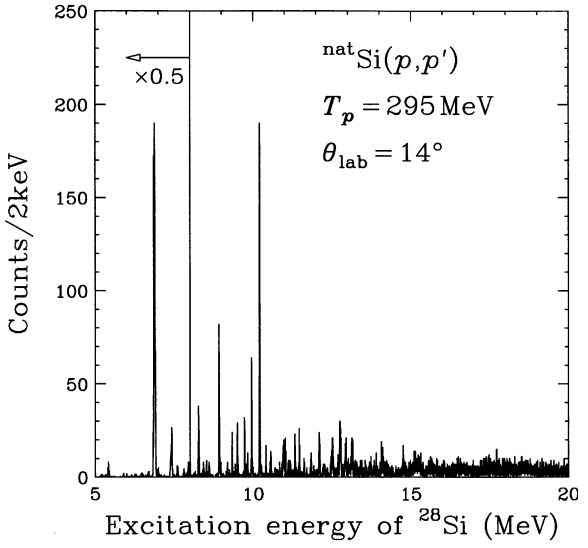

Fig. 10. Overall excitation energy spectrum of the ^{nat}Si(p, p′) scattering at $T_p = 295$ MeV and $\theta_{lab} = 14^\circ$ measured with the Grand Raiden spectrometer after employing the dispersion matching method.

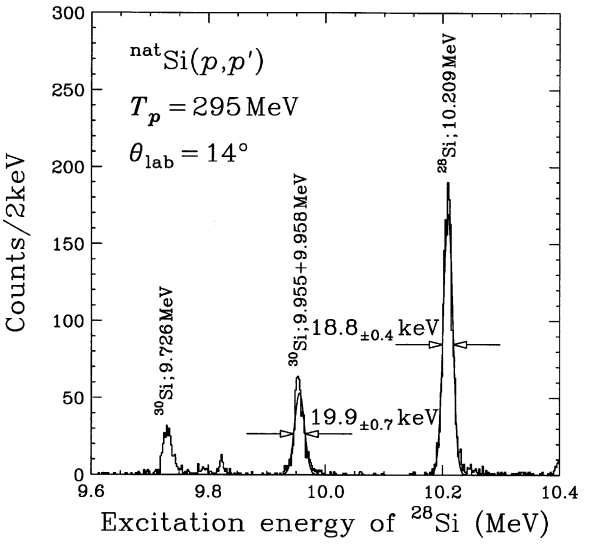

Fig. 11. Result of Gaussian peak-fitting for the ^{nat}Si(p, p′) scattering at $T_p = 295$ MeV and $\theta_{lab} = 14^\circ$. The overall energy resolution is 19.1 keV FWHM.

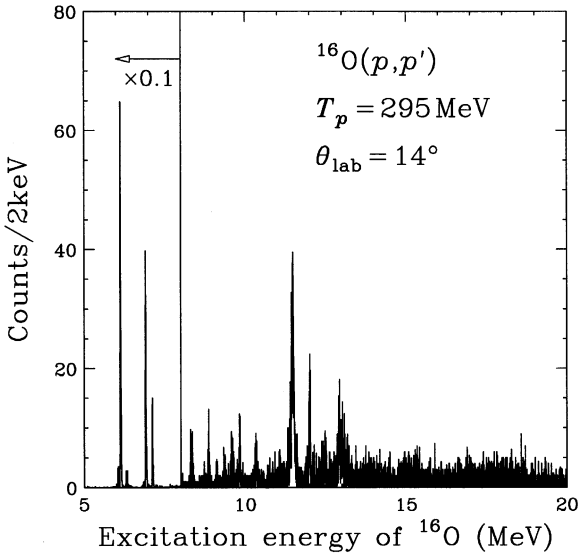

Fig. 12. Overall excitation energy spectrum of the $^{16}O(p, p')$ scattering at $T_p = 295$ MeV and $\theta_{lab} = 14°$ measured with the Grand Raiden spectrometer after employing the dispersion matching method.

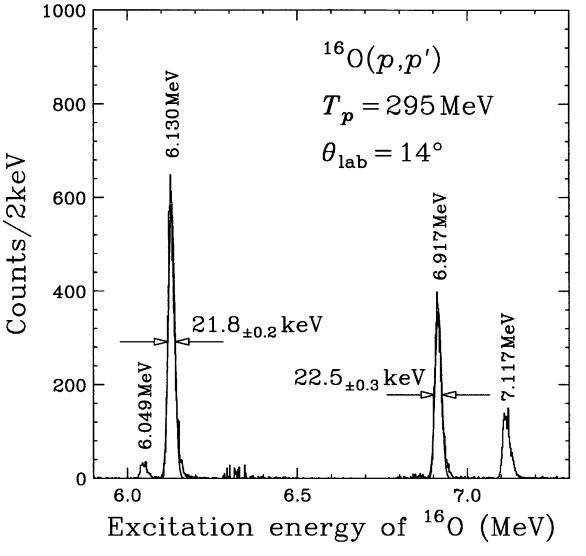

Fig. 13. Result of Gaussian peak-fitting for the $^{16}O(p, p')$ scattering at $T_p = 295$ MeV and $\theta_{lab} = 14°$. The overall energy resolution is 22.0 keV FWHM.

(see Fig. 13). The K value for ^{16}O is about -0.020, and x in Eq. (1) depends on θ_0 as $x = 0.32\theta_0$ after the kinematical correction of $s_{12} = -s_{16}K$. This means that the beam emittance of $\Delta\theta_0 = 1.1$ mrad contributes to Δx with 0.36 mm for ^{16}O. Furthermore, the effective magnification of $s_{11}b_{11}T + s_{12}b_{21}$ becomes larger by a factor of 1.3. These contributions to the energy resolution become about 20 keV which agrees fairly well with the experimental result of 22.0 keV.

9. Summary

The high resolution WS beam line has been designed and constructed to accomplish complete matching including both lateral and angular dispersion and focus matching with the high-resolution Grand Raiden spectrometer at RCNP. The WS beam line consists of six dipole magnets with a total bending angle of 270°. This beam line can be divided into five sections. The beam is focused in both the horizontal and vertical planes at the end of each section. The beam line polarimeter systems are positioned at the ends of first and second sections to measure all polarization components of the beam. They are separated by a bending angle of 115°, allowing the determination of horizontal components of the beam polarization. In dispersive mode, lateral and angular dispersions of the WS beam line are $b_{16} = 37.1$ m and $b_{26} = -20.0$ rad, necessary to satisfy dispersion matching conditions for Grand Raiden. The magnifications of the beam line are $(M_x, M_y) = (-0.98, 0.89)$ and $(-1.00, -0.99)$ for dispersive and achromatic modes, respectively.

The performance of the WS beam line was studied by using the faint beam method for the $^{168}Er(p, p')$ scattering. The WS beam line was successfully tuned to establish complete matching with Grand Raiden. We have succeeded to separate the first excited 2^+ state of ^{168}Er at $E_x = 79.8$ keV clearly from the ground state in the (p, p′) scattering. The achieved energy resolutions are $\Delta E = 13.0 \pm 0.3$ and 16.7 ± 0.3 keV in FWHM for 295 and 392 MeV protons, respectively. These energy resolutions agree well with the resolving power limit of the high-resolution Grand Raiden spectrometer.

Acknowledgements

We are grateful to the RCNP accelerator group for their help in various stages of construction and R/D. We also thank Professors H. Ejiri and Y. Nagai for their continuous encouragement throughout the work, and the RCNP Ring Cyclotron crew for their efforts in providing a good quality beam. We greatly thank Professor J. Cameron for donating the decommissioned IUCF K600 dipole magnets. The experiments were performed at RCNP by using R/D beam time and also under Program Number E155. This work was supported in part by the Grant-in-Aid for Scientific Research No. 12740151 of the Ministry of Education, Science, Sports and Culture of Japan.

References

[1] M. Kondo, et al., in: W. Joho (Ed.), Proceedings of the 7th International Conference on Cyclotrons and their Applications, Zürich, 1975, Birkhäuser, Basel, 1975, p. 95.
[2] I. Miura, et al., in: J.C. Cornell (Ed.), Proceedings of the 13th International Conference on Cyclotrons and their Applications, Vancouver, 1992, World Scientific, Singapore, 1993, p. 3.
[3] M. Fujiwara, et al., Nucl. Instr. and Meth. A 422 (1999) 484.
[4] M. Yosoi, et al., AIP Conf. Proc. 343 (1995) 157.
[5] J.M. Moss, Phys. Rev. C 24 (1982) 727.
[6] M.A. Franey, W.G. Love, Phys. Rev. C 31 (1985) 488.
[7] F. Osterfeld, Rev. Mod. Phys. 64 (1992) 491.
[8] A. Tamii, et al., Phys. Lett. B 459 (1999) 61.
[9] Y. Fujita, et al., Nucl. Instr. and Meth. B 126 (1997) 274.
[10] B.L. Cohen, Rev. Sci. Instr. 30 (1959) 415.
[11] S.A. Martin, et al., Nucl. Instr. and Meth. 214 (1983) 281.
[12] M. Berz, K. Joh, J.A. Nolen, B.M. Sgerrill, A.F. Zeller, Phys. Rev. C 47 (1993) 537.
[13] http://www.jlab.org/Hall-A/equipment/HRS.html
[14] P. Vernin, J. Le Bars, H. Fonvieille, G. Quéméner, J.J. LeRose, J. Hogan, B. Vlahovic, J. Billan, Nucl. Instr. and Meth. A 449 (2000) 505.
[15] T. Noro, et al., RCNP Annual Report, 1990, p. 217.
[16] T. Noro, et al., RCNP Annual Report, 1991, p. 177.
[17] H.G. Blosser, et al., Nucl. Instr. and Meth. 91 (1971) 61.
[18] H. Ikegami, et al., Nucl. Instr. and Meth. 175 (1980) 335.
[19] G.P.A. Berg, et al., IUCF Science and Technical Report 1986–1987, p. 152.
[20] K.L. Brown, et al., SLAC Report No. 91 Rev, 1, 1974, unpublished.
[21] K. Hatanaka, et al., RCNP Annual Report, 1991, p. 167.
[22] K. Hatanaka, et al., RCNP Annual Report, 1990, p. 209.
[23] Y. Fujita, et al., J. Mass Spectrom. Soc. Jpn. 48 (2000) 306.
[24] H. Fujita, et al., RCNP Annual Report, 1999, p. 87.
[25] T. Wakasa, et al., RCNP Proposal No. E155, 2000, unpublished.
[26] M. Uchida, et al., RCNP Proposal No. E156, 2000, unpublished.
[27] Y. Shimbara, et al., RCNP Proposal No. E158, 2000, unpublished.
[28] J. Rapaport, et al., RCNP Proposal No. E159, 2000, unpublished.
[29] G.P.A. Berg, et al., RCNP Proposal No. E163, 2000, unpublished.
[30] T. Wakasa, et al., RCNP Annual Report, 1999, p. 95.